

# The Remote Sensing Monitoring Analysis Based on Object-Oriented Classification Method

HaiJun Wang<sup>1</sup>, ShengPei Dai<sup>2</sup>, and Xiao Bin Huang<sup>1</sup>

<sup>1</sup> Engineering & Technical College of Chengdu University of Technology,  
614007 Leshan, China

<sup>2</sup> Institute of Scientific and Technical Information,  
Chinese Academy of Tropical Agricultural Sciences (CATAS),  
571737 Danzhou, China  
wanghaibo.2006@163.com

**Abstract.** In this paper, based on multi-temporal remote monitoring technology, using object-oriented classification method to monitor the change of vegetation of Zhangye oasis from TM/ETM data in 1989, 2000, 2011 years. The results show that: (1) the multi-resolution segmentation converted the single cell which had the similar texture, spectrum and shape to the object. Integrating nearest neighbor classifier and membership classifier to class the three data, and the overall accuracy of classification was 89.5%, Kappa coefficient was 0.9. The classification stability was 0.45 and 0.47 in 2000 and 2011 years. It showed that object-oriented classification method accuracy is higher than traditional classification method. (2)The three classification results indicate the area of bare land was larger than other, and it was reducing, with a percentage was 73.21%, 64.76%, 60.17%. The vegetation mainly distributed in both sides of Heihe River, the percentage of three data were 16.01%, 29.9%, 33.6%. The saline land was mainly distributed in the northwest of the oasis region, the percentage dropped to 2.33% from 4.89% during 1989 and 2011 years. (3) NDVI of the upstream was higher than the NDVI of the downstream on sides of river, the NDVI raised and the maximum value was 0.54. NDVI increased significantly from 1989 to 2011 years in Linze central region, and the maximum value reached to 0.58 in 2011 years, and it had the same characteristic in the southeast of Ganzhou district. The average NDVI of 2011 years was higher than in 2000 and 1989.

**Keywords:** Object-oriented Classification, Multi-resolution Segmentation, Remote Sensing Monitoring, Hexi Corridor, Accuracy Assessment.

## 1 Introduction

Vegetation plays a very important role in carbon-water-energy cycle of terrestrial ecosystems [1]. Vegetation is a bond that links soil, climatic, hydrologic and other elements in the whole ecosystem [2], but also an indicator of global climate change through carbon cycle [3]. Many scholars researched the relationship between vegetation and climatic factors [4], [5], [6], and it shows that: Vegetation cover

change is influenced by the climate change and atmospheric CO<sub>2</sub> fertilization effect in the long term [7], and it was influenced by the human activity directly or indirectly [2]. Therefore, the study on the relationship between vegetation and climatic factors became a core content in the International Geosphere Biosphere Program (IGBP), and it has very important significance to resource development and ecological environment protection.

Since the 1980s, the climate and environment of the Northwest China has changed significantly [8], especially in recent years, the precipitation in the Zhangye oasis and runoff in the Heihe river has changed significantly, its lead to changes of the region ecosystem and landscape. Under the condition of global warming, mainly in northwest China the climatic transformation from warm-dry to warm-wet happened in 1987 [9], and the air temperature was significantly high [10], and the precipitation was significantly increased in western Xinjiang [11] and the Qilian Mountains [9]. Many scholars have studied the status of ecological environment changes in these areas [12]. However, a few studies considered the use of remote sensing data in these areas [12]. To document the status and causes of change, it is important to utilize satellite images to assess vegetation change in Zhangye oasis. It can be revealed that the ecological environment change from detects of vegetation change based on remote sensing data. In this paper, the latest research progress of ecological change theory [13] was used to extract vegetation cover pattern from remote sensing data. The spatio-temporal variation of vegetation cover in Zhangye oasis agriculture zone was detected under the background of above mentioned, and then the natural and human driving factors of the vegetation changes over Zhangye oasis were discussed.

## 2 Materials and Methods

### 2.1 Materials

Data used in this study are as follows: (1) Three cloud-free Landsat TM/ETM images (path=133, row=33, acquired at Aug08 1989, Aug15 2000, Aug15 2011, respectively) were used for the present study with 28.5m × 28.5m spatial resolution and seven spectral bands (blue 0.45-0.52μm, green 0.52-0.60μm, red 0.63-0.69μm, near-infrared 0.76-0.90μm, mid-infrared 1.55-1.75μm, thermal infrared 10.40-12.50μm, mid-infrared 2.09-2.35μm) from the United States Geological Survey (<http://glovis.usgs.gov>). The vegetation cover of oasis area was best in the end of the summer. Therefore, the acquisition of images should be in the best leaf cover period, because the abundant leaf cover will improve the reflectance values recorded by remote sensing satellite. The three images were acquired on August within the best leaf cover period in the end of the summer. (2) The Land use data were the 1 km × 1 km spatial resolution land-use data in 2000 from the Environmental & Ecological Science Data Center for West China (<http://westdc.westgis.ac.cn/>). (3) The basic geographic information data in study area from National Geomatics Center of China (<http://ngcc.sbsm.gov.cn/guide/>). (4) The classification accuracy verification data from Google Earth image data (Google Inc., <http://www.google.com>) and field survey data.

## 2.2 Image Preprocessing

For image classification and change detection, we conducted relative radiometric calibration and Atmospheric calibration of Aug08 1989, Aug15 2000, Aug15 2011 images firstly. Then the first images were re-projected into a Universal Transverse Mercator (UTM) geographic coordinate system and were geometrically corrected by using ground control points (GCPs) gathered from pseudo-invariant targets in topographic maps such as road intersections, bridges, and other easily identified landmarks. Nearest neighbor resampling was used in all the geometrical transformations to minimize statistical properties change of the data sets [14]. A second order of polynomial transformation equation was used to re-project the images with a root mean square error (RMSE) of less than 0.5 pixels based on these control points. The corrected TM image was further used as reference image to register the rest two images [15]. Thirdly, the three images were linear stretch, enhancement and false-color composite (Fig. 2). The remote sensing software and data processing software used in this study was ENVI 4.8 for windows developed by the ITT Visual Information Solution (ITT Visual Solutions Inc., <http://www.ittvis.com/>) and ArcGIS 10 (ESRI Inc., <http://www.esri.com/>).

## 2.3 General Procedure and Image Segmentation

The procedures of this study are as show in figure 1 and as follows:

First, we implemented image segmentation and object classification in eCognition Developer 8.7 by building rule-sets that were applied to each image. In classification we considered the following major general land cover types of study area: Vegetation (Farmland and Forest land), Water, Construction land, Saline land and Bare land . Then we conducted post-classification change detection and accuracy assessment in ArcGIS 10 (ESRI Inc.) and further evaluated spatial distribution and classification stability.

To segment each image into small prototype objects we used eCognition multiresolution segmentation tool because in a heterogeneous natural landscape “meaningful” spectrally homogeneous objects can occur at different spatial scales [16]. Because varying farmland and forest land could emphasize the variation of spectral reflectance in the infrared and near-infrared region, and the vegetation foliage in the red band has a strong absorption characteristics. We gave higher weight to infrared and near-infrared band than to others.

To select the most suitable segmentation, we assessed the output sensitivity to multiple combinations of shape, scale and compactness [17] (Fig. 2) and set most appropriate parameters through repeated training area of interested (AOI) as the following steps:

- 1) Analyze the number of the land cover types and the size of the coverage area in the study area;
- 2) Set the scale factor, and then adjust the shape and compactness factor;
- 3) In the case of segmentation results are consistent with the actual feature, set the shape factor when fixed the compactness factor, vice versa.

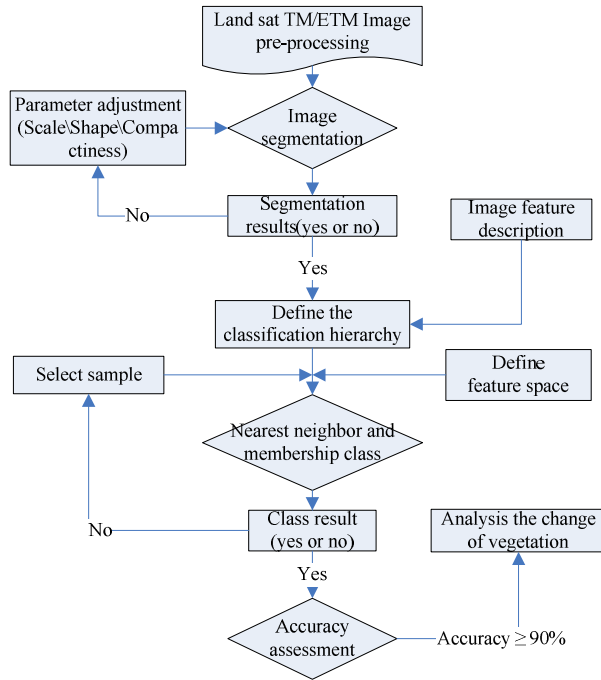


**Fig. 1.** The outline of study procedures

The segment must follow the following two principles:

- 1) To distinguish between the different areas of the image as much as possible to the maximum possible segmentation scale;
- 2) Meet the necessary shape standards as far as possible to use compactness factor. Because the most important information of the image data is the spectral information and higher weight of the shape factor will reduce the quality of the segmentation results.

## 2.4 Object-Based Classification

### Training Sample Selection

The training sample selection is based on the premise that our chosen classes are distinct cover types show in table 1, appropriate for the given image spatial resolution. The most “representative” objects for a class selected not only reference texture features in the image, but also need to refer to the spectral information. So, we were selected training samples from the initial segmentation result, which can distinguish the class and types to our knowledge and class description show in table 1, but this method is not accurate to “mixed” objects containing other classes. Therefore, the spectral characteristics of images must be use in the study, such as the spectral indexes (SIS) or band transformations.

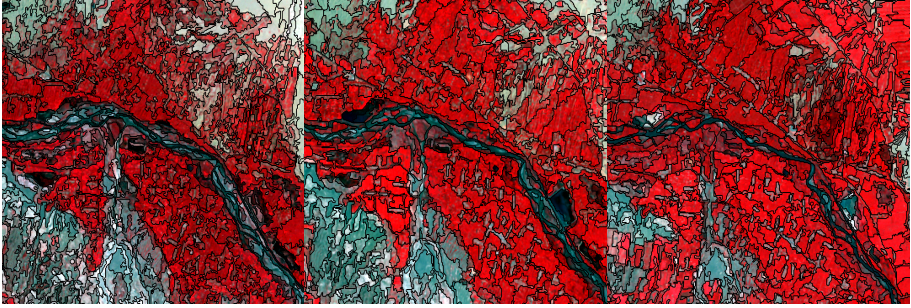


**Fig. 2.** The result of multi-resolution segmentation of AOI region in Zhangye Oasis (a. shape: 0.2, scale: 30, compactness: 0.5; b. shape:0.2, scale:30, compactness:0.5; c. shape:0.1, scale:25, compactness:0.6).

Hence one may assume that the most “representative” objects for a class are located close to the extremes of the spectral indexes (SIS) or band transformations which highlight that class most effectively. Specifically, we used Normalized Difference Vegetation Index [18] to represent Vegetation (farmland and forest land), where higher object-level NDVI values indicated a higher probability of a vegetation object. Likewise, Normalized Difference Water Index [19] represented Water, with higher NDWI suggesting higher chance of a water object.

Importantly, to determine which objects with the highest values of a respective index should be included in the training set, we needed to specify a cutoff threshold value for the index so that training objects could be selected from a pool of objects above that threshold value. The latter should be low enough so that the range of index values above the threshold is representative of the corresponding class, while also high enough to minimize the risk of including “mixed” objects containing other classes [20].

### **Classification and Change Detection**

The supervised classification based on samples and the fuzzy classifications based on spectral were used to classification. Based on the characteristics of the land cover types and the main object of this study area, we considered the following major general land cover types of study area: Vegetation (Farmland and Forest land), Water, Construction land, Saline land and Bare land. Next, we performed a three-step classification of the study area. First, using selected training objects and the spectral characteristics for Vegetation (Farmland and Forest land) and Water, we classified the area into these three classes. Second, we used all unclassified objects to determine training segments for other classes. The nearest neighbor supervised classification method was used to classify the construction land and saline land. Then, the unclassified objects were classified to bare land.

Finally, we repeated classification of the whole study area into five classes for each images and updated object class membership values. Applying our e-Cognition rulesets to each images separately helped to select training samples for different

classes in proportion to the class areas. Next, we analyzed the change among the major cover types between successive images in 1989, 2000, 2011 in Arc GIS 10.0 software.

## 2.5 Accuracy Assessment

### Confusion Matrix

In this paper, the confusion matrix was used to verify the accuracy of three classification results. For classification accuracy assessment, from each image we used approximately 30% of reference objects which represented Vegetation (farmland and forest land) as the primary class, ~20% objects - primarily water, 30% objects - primarily Saline land, ~10% objects - primarily Construction land and ~10% objects - primarily bare land. Because of the sampling data can not be covered panoramic images. These reference objects were assigned for each segmented image using field data obtained from the fund of the National Natural Science Foundation of China (NO. 40961038) and the supplementary information from Google Earth image data.

### Fuzzy Classification Stability Assessment

In order to account for high spatial heterogeneity of the study area, we conducted fuzzy classification stability assessment [21]. Each object has a classification probability value, and the difference between best and second best classification probability value means the object's fuzzy classification stability. The accuracy of classification results is highest, when the fuzzy classification stability value of an object is 1, and the accuracy of classification results is lowest, when the fuzzy classification stability value of an object is 0.

## 3 Results and Discussion

### 3.1 Land Cover Changes

Three classification results were classified separately by the approach mentioned above based on the three Landsat images (Fig. 3). Overall, the largest proportion of the study area was bare land, and then the artificial vegetation (farmland and forest land) class was banded distribution in the both sides of Heihe river, the north of Linze county and center part of Ganzhou district.

In all three scenes, bare land was consistently the dominant cover type occupying about 73.21% of the study area during Aug08 1989, 64.76% of the study area during Aug15 2000 and slightly declining to 60.13% in Aug15 2011. But the area of vegetation (farmland and forest land), the second largest class, was rapidly increasing from 16.01% to 33.60% of the study area from Aug08 1989 to Aug15 2011. And the area of water was slightly declining from Aug08 1989 (5.4%) to Aug15 2011 (1.95%). The area of construction land was slightly increased from Aug08 1989 (0.49%) to Aug15 2000 (2.11%), but then declined to 1.96% of the area in Aug15 2011. The area of saline land and slightly declined from Aug08 1989 (4.89%) to Aug15 2000 (1.18%), but then increased to 2.33% of the area in Aug15 2011.

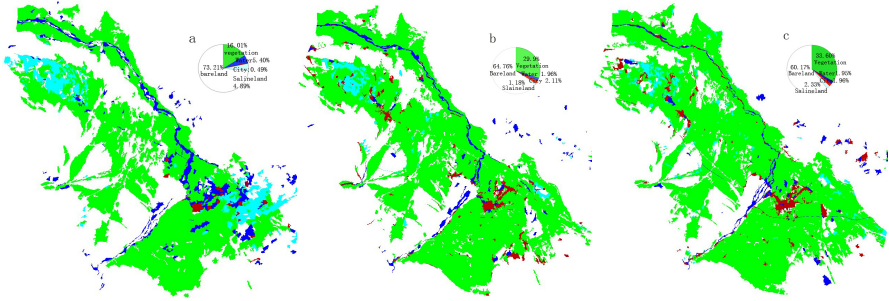


**Fig. 3.** The classification results of the study area (a. Aug08 1989; b. Aug15 2000; c. Aug15 2011)

### 3.2 Vegetation Change Detection

#### Spatial Distribution of Vegetation Changes

It shows the spatial distribution of vegetation change in study area from 1989 to 2011 (Fig. 4, Omission). During this time, the area of vegetation (farmland and forest land) was rapidly increasing in the southeast part of Ganzhou district and the north part of Linze County, and most of it was converted from saline land, woodland and waters. This implies that the ecological effect of ecological construction project has appeared.

#### The NDVI Changes from 1989 to 2011

The NDVI of three images was calculated by band algebra. In all three NDVI images, the NDVI has lower value in the center part of Linze County and the southeast part of Ganzhou district, because of low vegetation coverage in these areas.

The NDVI sampling data (average of  $20 \times 20$  cells) was obtained in two kilometers along the Heihe (Fig. 5a). There are same obvious undulating changes of the NDVI value from river upstream to downstream. The NDVI in both sides of the river upstream is higher than that in the river downstream. The NDVI value of river upstream is no difference in 1989, 2000 and 2011, but its value in 2011 was higher than that in 1989 and 2000 at river downstream. Overall, the NDVI was increased from 1989 to 2011, and that indicated the vegetation condition along the Heihe River was become better, and it may be related to the runoff of Heihe River (Liu, *et al.*, 2008).

The NDVI sampling data in Linze county and Ganzhou district shows an increase trend from 1989 to 2011 (Fig. 5b). The largest value was 0.44 in 1989, but that increased to 0.58 in 2011 in center part of Linze County. There is a same trend in southeast part of Ganzhou district from 1989 to 2011.

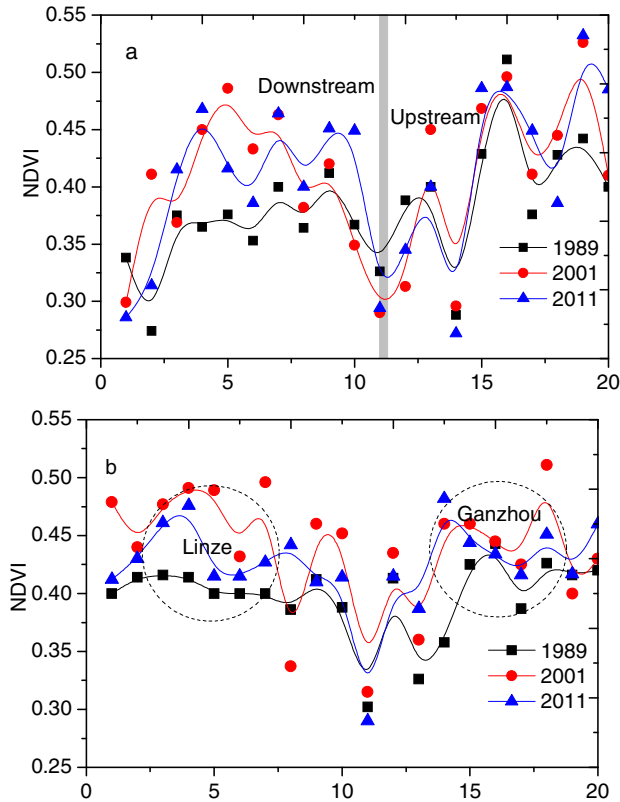


**Fig. 4.** The changes of sampling NDVI values from 1989 to 2011 (a. sampling in two kilometers along the Heihe river; b. sampling in Linze county and Ganzhou district)

### 3.3 Classification Accuracy

The final land cover classification scores high in the assessments of both overall accuracy and kappa coefficient. In 1989, 2000 and 2011, the overall accuracy and kappa coefficient was 86% and 0.85, 89% and 0.90, 90.8% and 0.92, respectively. Only a few misclassifications occur, and the overall accuracy of the object-based classification was higher the other methods [22], [23], [24], 25].

Fuzzy classification stability shows in the figure 6(Omission), and the color from green to red was represented the classification stability from high to low (Fig. 6 Omission). In 2000 and 2011, the average of the classification stability was 0.45, 0.47, and its highest was 1, 0.82, respectively, which shows a high accuracy of the classification (Table 1, Omission). But in contrast in 1989, the average and the highest of the classification stability was lower than that in 2000 and 2011 with 0.25, 0.75, respectively. The best membership assignments score generally high, the vegetation covers of the classification stability show the highest score in 1989, 2000 and 2011.



## 4 Conclusions

In this paper, the study presents an object-based classification of Hexi Corridor and change analysis of its general cover types during the 1989–2011. The three Landsat satellite images of 1989, 2000 and 2011 in Hexi Corridor were selected to get the vegetation change information. The temporal and spatial vegetation changes were analyzed and further evaluated spatial distribution and classification stability from 1989 to 2011. The main conclusions are as follows:

Our mapped classes represent spatially dominant components of the study landscape which shows the largest proportion of the study area was bare land, and then the artificial vegetation (farmland and forest land) class was banded distribution in the both sides of Heihe river, the north of Linze county and center part of Ganzhou district. The area of vegetation (farmland and forest land), the second largest class, was rapidly increasing from 16.01% to 33.60% of the study area from Aug08 1989 to Aug15 2011.

Our results suggest that changes in spatial distribution of major cover types largely followed the dynamics of the Heihe River. Vegetation was the most extensive class followed by Water. There are same obvious undulating changes of the NDVI value from river upstream to downstream. The NDVI in both sides of the river upstream is higher than that in the river downstream.

The final land cover classification scores high in the assessments of both overall accuracy and kappa coefficient, and the overall accuracy of the object-based classification was higher the other methods. The fuzzy classification stability shows the same trend. The best membership assignments score generally high, the vegetation covers of the classification stability show the highest score in 1989, 2000 and 2011.

## References

1. Cao, X.M., Chen, X., Bao, A.M.: Response of vegetation to temperature and precipitation in Xinjiang during the period of 1998–2009. *Journal of Arid Land* 3(2), 94–103 (2011)
2. Dai, S.P., Zhang, B., Wang, H.J.: Vegetation cover change and the driving factors over northwest China. *Journal of Arid Land* 3(1), 25–33 (2010)
3. Li, X.H., Shi, Q.D., Chang, S.L.: Change of NDVI based on NOAA image in northwest arid area of China in 1981–2001. *Arid Land Geography* 31(6), 940–945 (2008)
4. Tsuchiya, K., Igarshi, T., Qong, M.: Land cover change detection based on satellite data for an arid area to the south of Aksu in Taklimakan desert. *Journal of Arid Land* 2(1), 14–19 (2010)
5. Qian, Y.B., Zhang, H.Y., Wu, Z.N.: Vegetation composition and distribution on the northern slope of Karlik Mountain to Naomaohu basin, East Tianshan Mountains. *Journal of Arid Land* 3(1), 15–24 (2011)
6. Zhu, W.B., Lv, A.F., Jia, S.F.: Spatial distribution of vegetation and the influencing factors in Qaidam Basin based on NDVI. *Journal of Arid Land* 3(2), 85–93 (2011)
7. Xin, Z.B., Xu, J.X., Zheng, W.: Impact of climate change and human activities on the Loess Plateau in vegetation cover. *Science in China Series D: Earth Sciences* 37(11), 1504–1514 (2007)

8. IPCC (Intergovernmental Panel on Climate Change): Summary for policymakers of the synthesis report of the IPCC fourth assessment report. Cambridge University Press, New York (2007)
9. Shi, Y.F., Shen, Y.P., Li, D.L.: Discussion on the present climate change from warm-dry to warm-wet in Northwest China. *Quaternary Sciences* 23(2), 152–164 (2003)
10. Guo, Z.M., Miao, Q.L., Li, X.: Change characteristics of temperature in North China since recent 50 years. *Arid Land Geography* 28(2), 176–182 (2005)
11. Hu, R.J., Jiang, F.Q., Wang, Y.J.: A study on signals and effects of climatic pattern change from warm-dry to warm-wet in Xinjiang. *Arid Land Geography* 25(3), 194–200 (2002)
12. Zhang, J., Pan, X.L., Gao, Z.Q.: Estimation of net primary productivity of the oasis-desert ecosystems in arid west China on RS-based ecological process. *Arid Land Geography* 29(2), 255–261 (2006)
13. Méndez-Barroso, L.A., Vivonia, E.R., Watts, C.J.: Seasonal and inter annual relations between precipitation, surface soil moisture and vegetation dynamics in the North American monsoon region. *Journal of Hydrology* 377(1-2), 59–70 (2009)
14. Foody, G.M., Boyd, D.S., Cutler, M.E.J.: Predictive relations of tropical forest biomass from Landsat TM data and their transferability between regions. *Remote Sensing Environment* 85, 463–474 (2003)
15. Schowengerdt, R.A.: Remote sensing: models and methods for image processing. Academic Press (2006)
16. Blaschke, T., Lang, S., Lorup, E.: Object-oriented image processing in an integrated GIS/remote sensing environment and perspectives for environmental applications. In: Cremers, A., Greve, K. (eds.) *Environmental Information for Planning, Politics and the Public*, vol. 2, pp. 555–570. Metropolis, Marburg (2000)
17. Clinton, N., Holt, A., Scarborough, J.: Accuracy assessment measures for object-based image segmentation goodness. *Photogrammetric Engineering and Remote Sensing* 76(3), 289–299 (2010)
18. Tucker, C.J., Townshend, J.R.G.: African land-cover classification using satellite data. *Science* 227(4685), 369–375 (1985)
19. McFeeters, S.K.: The use of the normalized difference water index (NDWI) in the delineation of open water features. *International Journal of Remote Sensing* 17(7), 1425–1432 (1996)
20. Dronova, I., Gong, P., Wang, L.: Object-based analysis and change detection of major wetland cover types and their classification uncertainty during the low water period at Poyang Lake, China. *Remote Sensing of Environment* 115(12), 3220–3236 (2011)
21. Schneevogt, N.J., van der Linden, S., Kellenberger, T.: Object-oriented classification of alpine landforms from an ASTER scene and digital elevation data (Reintal, Bavarian Alps). *Grazer Schriften der Geographie und Raumforschung* 45, 53–62 (2010)
22. Yang, H.L., Peng, J.H.: Remote sensing classification based on Markov random field and fuzzy C-means clustering. *Acta Geodaetica et Cartographica Sinica* 41(2), 213–218 (2012)
23. Zhao, P., Fu, Y.F., Zheng, L.G.: Cart-based land use/cover classification of remote sensing images. *Journal of Remote Sensing* 9(6), 708–716 (2005)
24. Guo, L., Pei, Z.Y., Wu, Q.: Application of method and process of object-oriented land use-cover classification using remote sensing images. *Transactions of the CSAE* 26(7), 194–198 (2010)
25. Liu, Z.G., Shi, W.Z., Li, D.R.: Partially supervised classification of remotely sensed imagery using support vector machines. *Journal of Remote Sensing* 9(4), 36–372 (2005)